Contents

S1 Example Fayetteville Gathering Station with Compression and Dehydration (C/D Gathering Station)

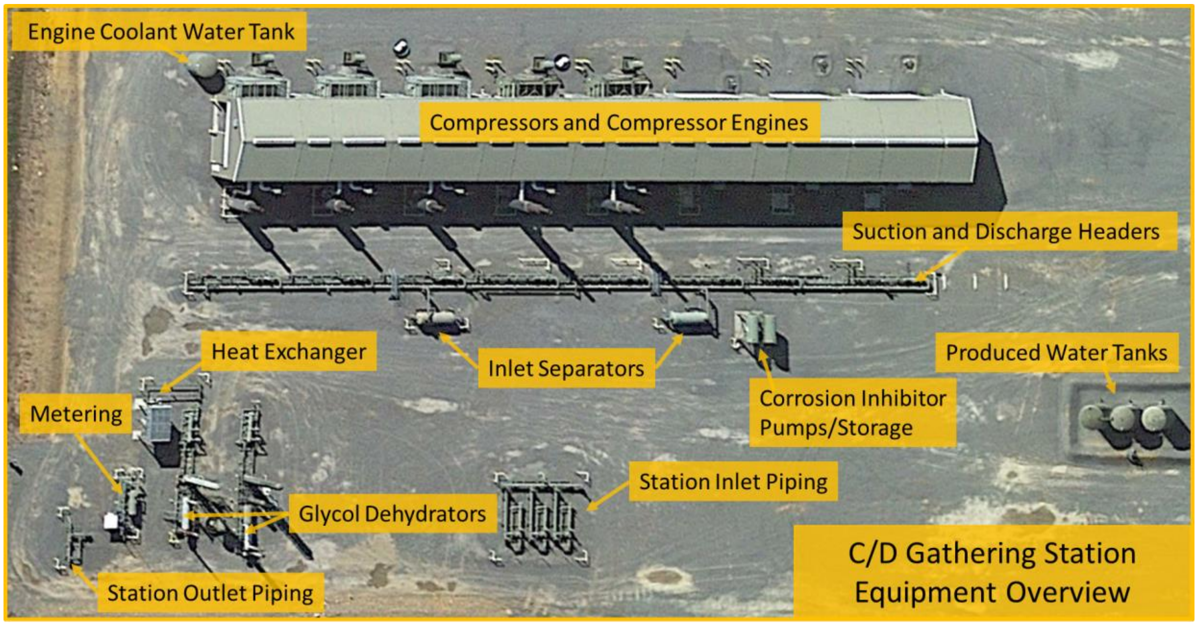

Figure S1: Gathering station aerial view. This gathering station included equipment for compression and dehydration of gas delivered from nearby wells.

At each measured gathering station on-site observers documented the operating state of compressor engines during measurement, and instantaneous total facility throughput where available. As shown in Figure S2 a strong correlation exists between these parameters.

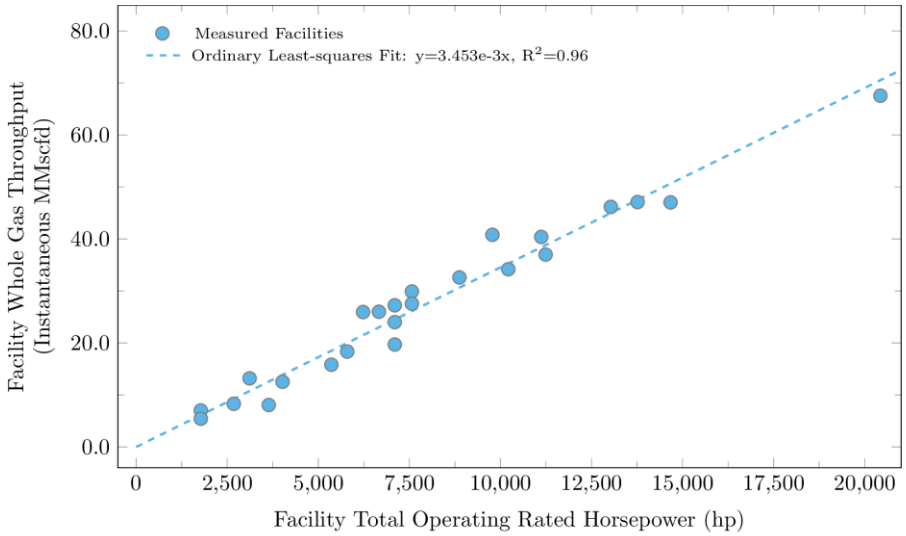

Figure S2: Total facility operating rated horsepower is directly correlated with facility throughput. On-site observers documented real-time facility throughput and compressor engine operating state during field measurements.

S2 Field Measurements and Protocol

The gathering station measurement protocol used in this study is outlined in 'Annex 3 Gathering Measurement Protocol' of the final report for RPSEA/NETL contract no 12122-95/DE-AC26-07NT42677. Figure S3 shows the study area (orange highlight) and all gathering stations within the study area. Measured gathering stations are highlighted.

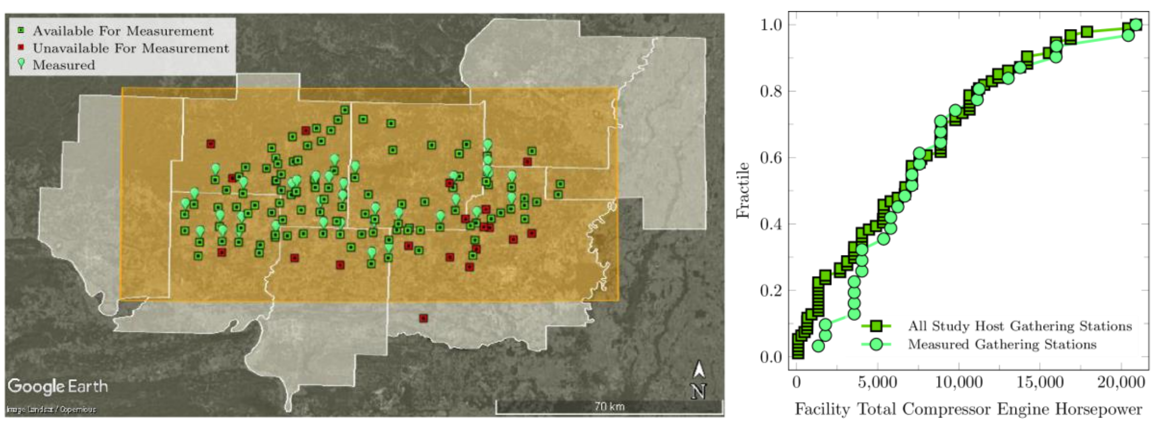

Figure S3: Ninety-nine out of 125 gathering stations within the study area (orange highlighted region) were available for measurement. Collectively, thirty-six stations were measured by, on-site, tracer, and aircraft teams (left). Considering the size of the stations, as estimated by installed compressor engine power, the measured are representative of all facilities available for measurement (right).

On-site measurements were made by AECOM, or AECOM and study partner personnel "on-site or on-site team". Tracer measurements were made by Aerodyne Research Incorporated

(Yacovitch et al., 2017) "tracer or tracer team", and Aircraft measurements were made by Scientific Aviation Incorporated (Conley et al., 2017) "aircraft or aircraft team".

Table S1: Availability of measurement teams during the field campaign.

	Campaign Week			
Team	1	2	3	4
Onsite Observer	✓	✓	✓	✓
AECOM/LDAR	✗	✓	✓	✓
Tracer Team	✓	✓	✓	✗
Aircraft Team	✓	✓	✓	✓

For detailed on-site measurement protocol, see 'Annex 4 Onsite Detection and Measurement Protocol' of the final report for RPSEA/NETL contract no 12122-95/DE-AC26-07NT42677.

S3 Data Tables

See the attached document 'SI_DataTables.xlsx'

S3.1 All Facilities Measured with SOE Results

See 'SI_DataTables.xlsx', Sheet 'S3.1-MeasResults'

S3.2 All Facilities Measured with Alternate SOE Results

Model results using SOEs developed using measured dehydrator regenerator vents. See 'SI_DataTables.xlsx', Sheet 'S3.2-AltSOEMeasResults'

S3.3 Measurement Date and On-site Observer Status

See 'SI_DataTables.xlsx', Sheet 'S3.3 -MeasDateObserver'

S3.4 On-site Direct Measurements

A summary of all on-site direct measurements (ODMs) collected at gathering stations during the field campaign. See 'SI_DataTables.xlsx', Sheet 'S3.4-OnsiteDirectMeas'

S3.5 Compressor Engine Exhaust Stack Test Data

A summary of study partner provided compressor engine exhaust stack test data. See 'SI_DataTables.xlsx', Sheet 'S3.5-CombSlip'

S3.6 G3606 Load Percent Observed During Field Campaign

At measured gathering stations using Caterpillar ®G3606 compressor engines, operating load was available on the display panel and was noted by on-site observers. See 'SI_DataTables.xlsx', Sheet 'S3.6-G3606FieldLoadPrcnt'

S3.7 Aircraft Spiral Flight Summary Data Table

See 'SI_DataTables.xlsx', Sheet 'S3.7 -AircraftData'

S4 Modeling Emissions: Study On-site Estimate (SOE) Component Categories

Study on-site estimates (SOEs) were developed for every gathering station measured by on-site measurement teams and are provided in S3. Comparison of SOEs to tracer and aircraft were performed as described in the main article.

S4.1 Simulated Combustion Slip

Combustion slip (unburned fuel entrained in engine exhaust) represents a significant component of total methane emissions at gathering stations. No measurements of combustion exhaust were made during the field campaign, but study partner companies provided recent exhaust stack test data. These data were measured by contractors who performed stack tests in accordance with standard protocol (EPA Method 19 (US EPA, n.d.), EPA Method 320 (US EPA, n.d.)) in the year prior to the field campaign (January to September, 2014). Stack test data were provided for 111 engines; 24 were from one engine series (Caterpillar® G3500, rated at ≈1 MW), and 87 from another (Caterpillar® G3600, rated at ≈1.3 MW). All compressor engines present at measured gathering stations belonged to one of these engine series.

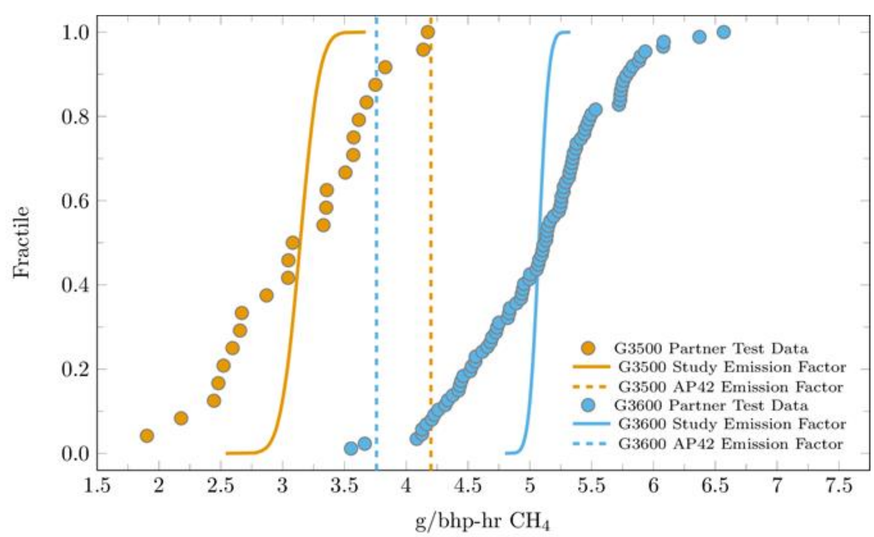

Figure S4: Compressor engine exhaust contributes a significant portion to methane emissions at gathering stations. Recent study partner stack test data provided improved estimates relative to aggregate emission factors.

Stack test data were normalized by the average brake horsepower of the engine during the test. Means and 95% confidence intervals developed from *n*-out-of-*n* bootstrap resampling for each engine series show statistically significant differences in mean combustion slip (G3500: mean 3.10 g CH_4/bhp-h (± 0.23); G3600: mean 5.02 (± 0.12) g/bhp-h). This is equivalent to 4.15 (± 0.32) kg CH_4/h and 8.9 (± 0.21) kg CH_4/h respectively, for each engine series when operating at rated power. These emission rates are similar to those recently measured by Johnson et al. (2015) at transmission compressor stations in the Barnett shale.

Table S2 compares emission factors and rates from this test data to three EPA methods: (1) greenhouse gas inventory (GHGI) (US EPA, 2016), (2) compilation of air pollutant emission factors (AP 42) (US EPA, n.d.), and (3) greenhouse gas reporting program (GHGRP) Subpart C (40 C.F.R. § 98.33, n.d.). Emission factor differences between methods and between engine types highlight the importance of using emissions measurements specific to the engine type to estimate emissions from activity data for each facility. For example, the AP-42 factor would overestimate combustion slip by 26% for measured G3500 series engines, and underestimate combustion slip from measured G3600 series engines by 34%, when assuming manufacturer rated fuel use at rated power.

Table S2: Combustion Slip Emission Factor Summary Table. EPA factors (GHGI, AP 42, Subpart C) assume manufacturer rated fuel use at rated power.

	G3500		G3600	
	Factor (g/bhp-h)	Rate (kg/h)	Factor (g/bhp-h)	Rate (kg/h)
Study	3.10 (+/- 0.23)	4.15 (+/- 0.32)	5.02 (+/- 0.12)	8.9 (+/- 0.21)
GHGI	4.62	6.19	4.62	8.2
AP 42	4.2	5.63	3.76	6.67
Subpart C	7.4e-3	9.9e-3	6.6e-3	11.8e-3

For each Monte Carlo iteration, *i,* combustion slip methane emissions for facility *j* are calculated as:

$$\dot{m}_{combustion\ slip,i} = \sum_{k=1}^{N_{op}} \text{draw}(EF_{series(k)}) * \text{draw}(Load_k) * RatedHP_k$$

Where:

N_{op} represents the count of compressor engines operating on-site during the measurement.

$\text{draw}(EF_{series(k)})$ indicates drawing one emission factor value at random from the distribution of emission factors for the same engine series as engine k.

$\text{draw}(Load_k)$ indicates drawing a fractional load at random from the distribution of operating loads observed during the field campaign, and applying it to engine k.

$RatedHP_k$ is the rated power output of engine k.

Emission factor distributions and observed operating loads as noted by on-site observers during the measurement campaign are provided in S3.

S4.2 On-site Direct Measurements (ODMs)

For each iteration *i* of the SOE model, methane emissions from ODMs at facility *j* are calculated as:

$$\dot{m}_{ODM,i} = \sum_{k=1}^{N} f_i * ODM_k$$

Where N is the number of on-site direct measurements made at facility *j* not subject to any emission rate exceptions, and f_i is a factor drawn at random from a normal distribution to account for the high-flow sampler instrument uncertainty (+/- 10%) (Bacharach, Inc., 2015).

Table S3: On-site direct measurements made by on-site teams during the field campaign. Some measurements were made at facilities not included in method comparisons. All valid measurements were included in distributions used in study on-site estimate development.

	Onsite Direct Measurements				Observations	
Equipment Type	Valid Measurement	Above Hi-Flow Range	Below Hi-Flow Range	Total Sources Measured	Observed Not Measured	Total Sources Observed
Compressor	208	5	80	293	16	309
Dehydrator	15	-	20	35	-	35
Other	26	-	26	52	2	54
Pig Launcher/Receiver	1	-	-	1	-	1
Piping or Gas Line	25	-	15	40	-	40
Separator	25	-	27	52	-	52
Tank	9	-	2	11	8	19
Total	309	5	170	**484**	26	**510**

A complete list of on-site device measurements including equipment type and component category is provided in S3.

S4.3 Simulated Direct Measurements (SDMs)

SDMs account for emission sources observed but not measured, or measurements above or below the measurable leak rate of the high-flow sampler.

$$\dot{m}_{SDM,j} = \dot{m}_{obsnotmeas,i} + \dot{m}_{abovehf,i} + \dot{m}_{belowhf,i}$$

Emissions observed but not measured at facility *j* are sampled from the distribution of ODMs developed during this study as

$$\dot{m}_{obsnotmeas,i} = \sum_{k=1}^{N_{ex}} \text{draw}(\dot{m}_{ODMeqptype(k)})$$

Where:

N_{ex} is the number of observed not measured methane emission sources

draw($\dot{m}_{ODMeqptype(k)}$) indicates drawing one value from the appropriate equipment type for emission source k

Emissions recorded at or above the measurable leak rate of the high-flow sampler were removed from the ODM category, and were estimated by drawing a replacement emission rate from a right triangular distribution with maximum probability at the maximum measurable leak rate of the high-flow sampler (8 SCFM, 9.24kg/h) (Bacharach, Inc., 2015), tapering to a minimum probability at an emission rate of 16 SCFM (18.48 kg/h), and added to the SDM category. Emissions observed with OGI, but recorded below the measurable leak rate of the high-flow sampler (0.05 SCFM, 0.058 kg/h) (Bacharach, Inc., 2015), were removed from the ODM category, and were estimated by multiplying the measured reading by an uncertainty factor that increased linearly from +/- 10% at the lower measurable leak rate to +/- 100% at recorded emission rate of 0 SCFM, and added to the SDM category. See S9.

S4.4 Measured Dehydrator Regenerator Vents

Dehydrator regenerator vents were not expected to be a significant methane emission source based on GRI-GLYCalc (GRI-GLYCalc Version 4.0, n.d.) simulations (an approved software program for predicting air emissions from glycol dehydrator units in 40 CFR 98.233) and a 1996 GRI study (Myers, 1996). However, a limited number of field measurements exhibited substantially larger methane emissions than predicted. Glycol dehydrators at one gathering station were equipped with passive condensers known as “BTEX Busters”, which cool the regenerator vent exhaust stream, thereby removing entrained liquids and volatile organic compounds. The regenerator vents on four dehydrator units were measured with the high-flow sampler at 7.6, 5.7, 5.2, and 1.2 kg/h respectively (see Table S4). The vents on these four units are the only sources that contribute to the measured dehydrator regenerator vent category.

S4.5 Simulated Glycol Dehydrator Regenerator Vents

Process simulations of dehydrator regenerator vent emissions using GRI-GLYCalc are highly sensitive to input parameters (Zavala-Araiza et al., 2017), and nullify regenerator vent emissions if the user indicates that the simulated unit employs flash tank vapor recovery (an emission control technique). All four dehydrator units measured in the field campaign employed flash tank vapor recovery, but measured methane emissions were larger than uncontrolled emissions predicted by GRI-GLYCalc and a 1996 GRI study (Myers, 1996). Dehydrator regenerator vents were simulated in method comparisons in the main article based on the GRI study emission factor for dehydrator units with flash tanks. Alternate method comparisons are provided in S5, where methane emissions from unmeasured glycol dehydrators were simulated based on the four measured units. Four emission factors were developed by normalizing the measured emissions by the rated horsepower of operating compressor engines providing gas to each unit. Gas throughput measurements were not available for individual dehydrator units; however, throughput is directly correlated to operating horsepower (see S1).

Simulation of dehydrator regenerator vent emissions proceeds as follows:

$$\dot{m}_{simdehyregen,i} = \sum_{k=1}^{N_{op}} \text{draw}(EF_{dehyregen(k)}) * \text{draw}(Load_k) * RatedHP_k$$

N_{op} represents the count of compressor engines operating on-site during the measurement.

draw$(EF_{dehyregen(k)})$ indicates drawing one emission value from the distribution of regenerator vent emission factors developed from measured dehydrator regenerator vents.

draw$(Load_k)$ indicates drawing a fractional load at random from the distribution of operating loads observed during the filed campaign, and applying it to engine k.

$RatedHP_k$ is the rated horsepower of engine k.

Table S4: Measured glycol dehydrator regenerator vent emissions on four units were substantially larger than those predicted by GRI-GLYCalc. Study emission factors are created based these measurements and the total operating compressor engine horsepower supplying gas to each unit.

Dehydrator:	Unit 1	Unit 2	Unit 3	Unit 4	
Rated Compressor Power Input	5325	5325	5325	3115	hp
Flow from Correlation	18.4	18.4	18.4	11.2	MMscfd
Measured Regenerator Vent	7.6	5.7	5.2	1.2	kg/h
GRI-GLYCalc Controlled Regenerator Vent	0.04	0.04	0.04	0.02	kg/h
GRI-GLYCalc Uncontrolled Regenerator Vent	0.72	0.72	0.72	0.42	kg/h

S4.6 Simulated Compressor Engine Crankcase Vents

Simulated Crankcase Vents account for CH_4 vented from compressor engine crankcase vents because of imperfect piston ring sealing. Crankcase vents on compressor engines were not measured in this study, but were simulated based on a Caterpillar® crankcase ventilation application guide (Caterpillar, n.d.), which stated that crankcase hydrocarbon emissions are normally 3% of exhaust emissions at engine mid-life, but could be as high as 20% due to engine wear. Crankcase emissions were calculated in the Monte Carlo model for method comparisons in the main article by multiplying combustion slip emissions by a factor drawn at random from a normal distribution (mean 3%, assumed standard deviation 2%).

In the alternate method comparisons in S6, simulated dehydrator regenerator vents were calculated using recent measurements from Johnson et al. (2015). They measured crankcase vent methane emissions and combustion slip on Caterpillar® 3500 and 3600 series compressor engines and found crankcase vent emissions were 14.4% of combustion slip on average (range 7% -22%).

Simulation of compressor engine crankcase vent emissions proceeds as follows in the alternate analysis presented in S6:

$$\dot{m}_{simcrankvent,i} = \sum_{k=1}^{N_{op}} \text{draw}(EF_{simcrankvent(k)}) * \dot{m}_{combustion\ slip,i}$$

N_{op} represents the count of compressor engines operating on-site during the measurement.

$\text{draw}(EF_{simcrankvent(k)})$ indicates drawing one value from the distribution of crankcase vent emissions as a fraction of combustion slip emissions from Johnson et al. (2015).

$\dot{m}_{combustion\ slip,i}$ indicates the combustion slip calculated for engine k calculated in Monte Carlo iteration i.

S5 Paired Measurements Excluded from Comparisons

S5.1 Gathering Station 61

At gathering station 61, substantial portions of the facility were not covered for leak detection via OGI. Therefore, SOE is not accepted at this facility due the potential for unidentified emission sources which would have contributed to the tracer measurement, and not the SOE at this facility, preventing a fair comparison. Therefore, this facility is eliminated from the:

- Tracer and Study On-site Estimate method comparison

S5.2 Gathering Station 121

Significant emissions were identified by the aircraft during a raster flight as originating from gathering station 121. Gas was venting from a produced water tank, which originated from an open manual (hand-operated) dump valve on a compressor engine fuel scrubber. On-site teams were unable to measure the emissions from the tank, which were above the measurement range of the high-flow sampler. The tracer team was not able to provide a facility-level emission rate (FLER) due to poor winds and downwind road access, but could isolate the portion of the facility where the tank was located, both with the valve open, and after it had been identified and closed. By subtracting the tracer estimate made in each operating state, and subtracting the associated uncertainties (95% CI) in quadrature, tracer estimates 606 (+/- 278 kg/h) originating from the tank. Aircraft facility estimates were performed at this facility on three different days: on two days measurements captured the facility in a higher emitting state 676 (+/- 119 kg/h), and 739 (+/- 107 kg/h), and on one day at a lower emitting state 276 (+/- 99 kg/h). If the tank emissions estimated by tracer are added to the SOE at this facility 109.6 (-8.1/+7.9 kg/h), the SOE compares well with the aircraft on the two days the aircraft captured the facility in a higher emitting state.

This facility was selected for measurement by directed, and not random sampling. The on-site team was not able to measure the tank emissions; the tracer team was not able to produce a complete FLER due to poor wind conditions; the aircraft captured the facility in multiple (high) emitting states, showing high variability. Aircraft measurements were not made concurrently with tracer or on-site measurements. Therefore, this facility is excluded from the:

- Tracer to Study On-site Estimate method comparison
- Aircraft to Study On-site Estimate method comparison

S5.3 Gathering Station 33

Significant emissions were noted from a produced water tank, which were likely above the range of the high-flow sampler, and which the on-site team therefore did not attempt to measure. Study partner company operators suspected a stuck dump valve, but were unable to identify the source during the time the measurement was conducted. At this facility, tracer measurements would include emissions from the tank that the on-site team was unable to measure, and had no way to quantify or otherwise estimate with any degree of certainty. Therefore, this facility is excluded from the:

- Tracer to Study On-site Estimate method comparison

S5.4 Gathering Station 111

During measurements at gathering station 111, an operating compressor was accidentally shut down, and operators had trouble restarting it due to water in the fuel line. The fuel line was vented and purged, and the compressor piping was vented and purged multiple times. After several attempts the compressor engine was restarted, and normal operations resumed. On-site teams did not measure these large, non-continuous emissions, and tracer teams captured them, reporting highly variable emissions, with periods of high and unsteady concentration enhancements seen just downwind of the facility. The aircraft measured this facility 30 minutes after the compressor engine was restarted. Therefore, this facility is excluded from the:

- Tracer to Study On-site Estimate method comparison
- Aircraft to Study On-site Estimate method comparison

S5.5 Gathering Station 96

It was determined from a post-campaign activity data survey that a manual unloading had occurred at a well within the flight path during an aircraft spiral flight targeting a nearby gathering facility. Theses emissions would have contributed to aircraft measurements, and would not have contributed tracer measurements or SOE.

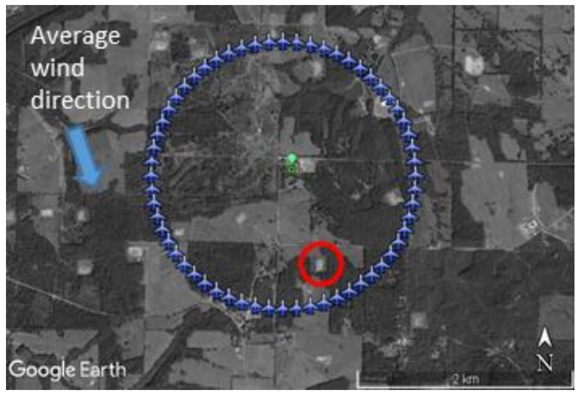

Figure S5: A well (red circle) underwent a manual unloading during aircraft measurements targeting a gathering station at the center of the aircraft flight (green balloon).

Therefore, this facility is excluded from the:

- Aircraft to Study On-site Estimate method comparison

S5.6 Gathering Station 98

During post-campaign quality control, it was determined that completion work was being performed on a well immediately upwind from the aircraft flight path. These emissions provided a confounding upwind source for the aircraft.

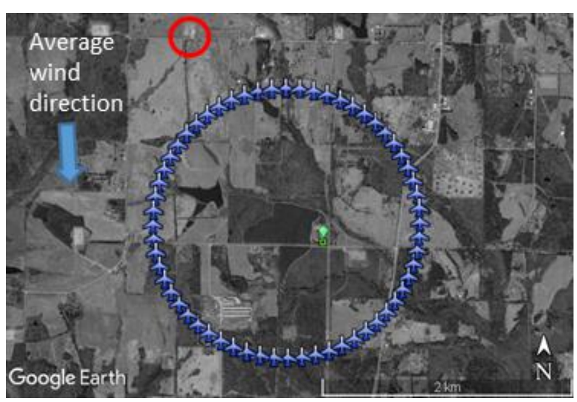

Figure S6: A well (red circle) was undergoing completion work during aircraft measurements targeting a gathering station (green balloon), confounding measurements.

Therefore, this facility is excluded from the:

- Aircraft to Study On-site Estimate method comparison

S6 Alternate Method Comparisons Using SOEs Developed from Measured Dehydrator Regenerator Vents

Section S6 reports results from alternate method comparisons that calculate simulated dehydrator regenerator vents based on 4 dehydrator units measured in this study. Additionally, compressor engine crankcase vents are calculated based on recent measurements by Johnson et al. (2015). All other SOE categories are calculated in the same way as they were for the method comparisons presented in the main article.

S6.1 SOE and Overall Results Summary

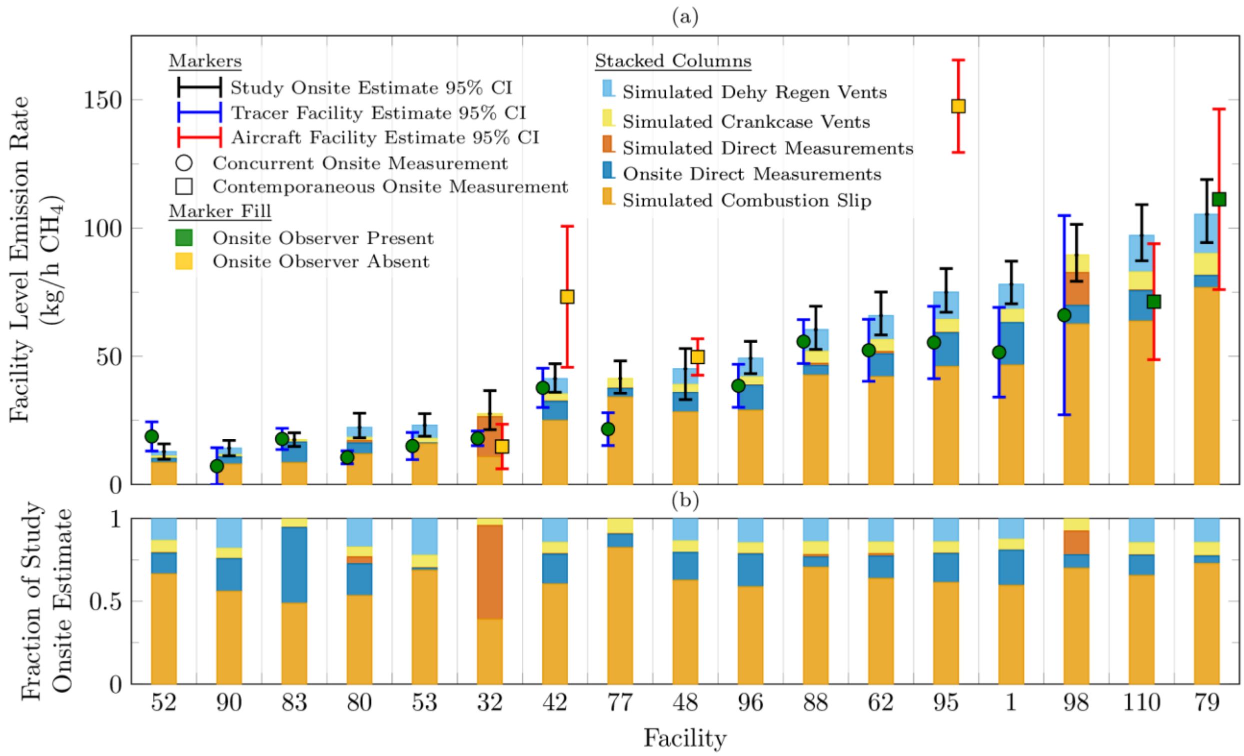

Figure S7: Facility-level CH_4 emission rate summary at all facilities included in method comparisons. Study on-site estimates (SOE) are the sum of on-site direct measurements plus engineering estimates for unmeasured sources (stacked columns, black error bars). Tracer (left mark, blue error bars) and aircraft (right mark, red error bars) are overlaid at facilities where these measurements were compared to SOEs. Marker shape and fill indicate same/different day and the presence/absence of on-site observers, which influence the comparability of measurements. Bottom panel illustrates the fraction of the SOE contributed by each component; combustion slip contributes more than half of emissions at 15 of 17 facilities and accounts for two thirds of cumulative SOE emissions for these 17 facilities.

Simulated Combustion Slip was the largest source category and contributed 63% to the cumulative SOE for the 17 facilities included in method comparisons shown in Figure S7. *ODMs* contributed 14%, *SDMs* contributed 5%, *Simulated Crankcase Vents* contributed 7%, and *Simulated Dehydrator Regenerator Vents* contributed 10% to the cumulative SOE.

For each measurement method, 95% confidence intervals indicate that the method would produce a FLER within the interval 95% of the time. We consider methods with overlapping confidence intervals to agree. Tracer and SOE 95% confidence intervals overlap at 10 out of 14 facilities, while aircraft and SOE confidence intervals overlap at five out of six facilities.

S6.2 Tracer Facility Estimate and Study On-site Estimate Comparison

When compared in aggregate by difference plot and variance-weighted least-squares regressions, tracer predicts lower FLER than SOE for 14 concurrently-measured gathering stations at the 95% confidence level (see Figure S8). In Figure S8(a) the difference of tracer and SOE is plotted against the uncertainty weighted mean of tracer and SOE. The mean of differences (termed "bias") is -10.9 kg/h, indicating that tracer predicts lower FLER than SOE. A paired t-test is used to determine if the bias is significant. The shaded area in Figure S8(a) highlights the 95% confidence interval on bias. The confidence interval does not include $x = 0$, which indicates that the bias is statically significant at the 95% confidence level. The "limits of agreement" are given by two standard deviations of method differences and provide an assessment of method agreement based on the measured data. The limits of agreement for tracer and SOE are ± 17.6 kg/h (dash-dot lines in Figure S8(a)), indicating that tracer may predict a FLER 28.5 kg/h less than or 6.7 kg/h greater than SOE.

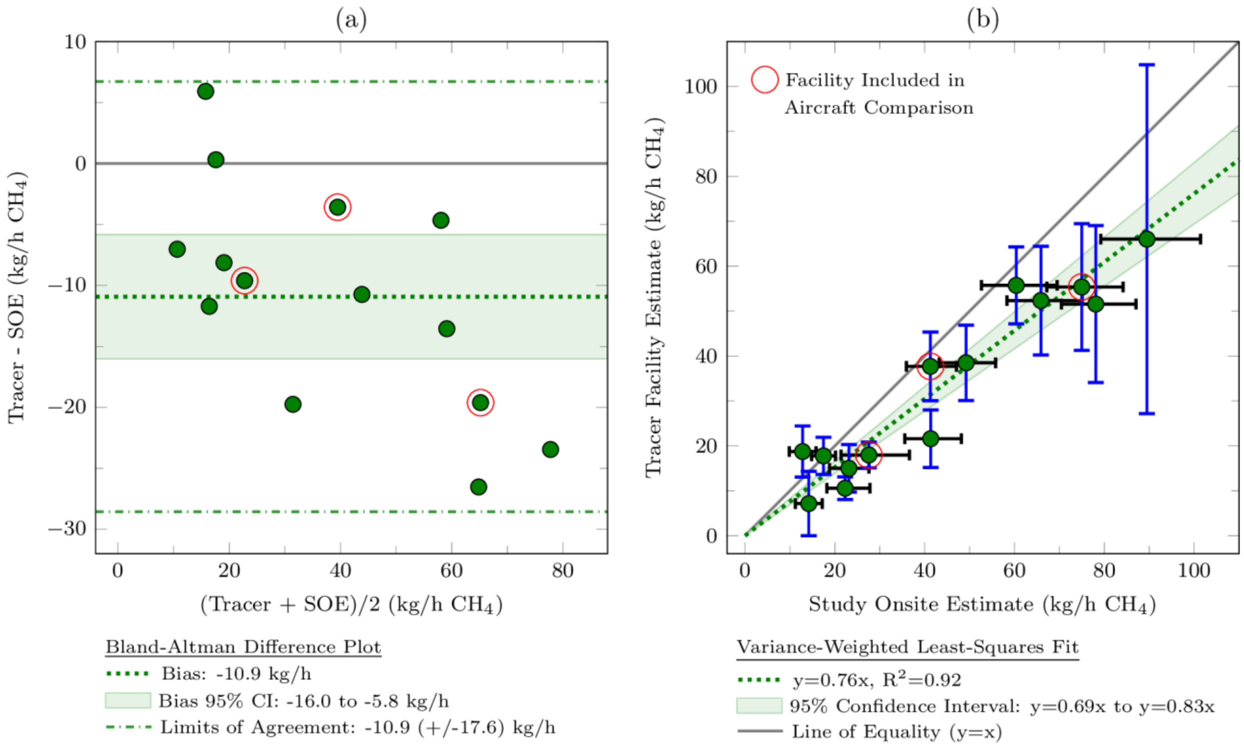

Figure S8: Tracer predicts lower facility-level CH4 emission rates than study on-site estimates at the 95% confidence level using (a) difference plots and (b) variance-weighted least-squares regressions.

In Figure S8(b) a VWLS regression (dashed line) is performed on tracer and SOE. The slope of the regression (tracer = 0.76·SOE, $R^2 = 0.92$) is less than unity, indicating that tracer predicts lower FLER than SOE. The 95% confidence interval (shaded region) on the regression slope (tracer = 0.69·SOE to tracer = 0.83·SOE) does not include the line of equality ($y = x$), indicating that tracer predicts lower FLER than SOE at the 95% confidence level.

S6.3 Aircraft Facility Estimate and Study On-site Estimate Comparison

Aircraft predicts higher FLER than SOE when compared by difference plot and VWLS regression, as shown in Figure S9. When compared by difference plot, aircraft is biased high relative to SOE (16.9 kg/h). However, the bias is not statistically significant because the 95% confidence interval includes $x = 0$. The limits of agreement for aircraft and SOE are ± 65.4 kg/h (dash-dot lines in Figure S9(a)), indicating that aircraft may predict a FLER 82.3 kg/h greater than or 48.5 kg/ h less than SOE.

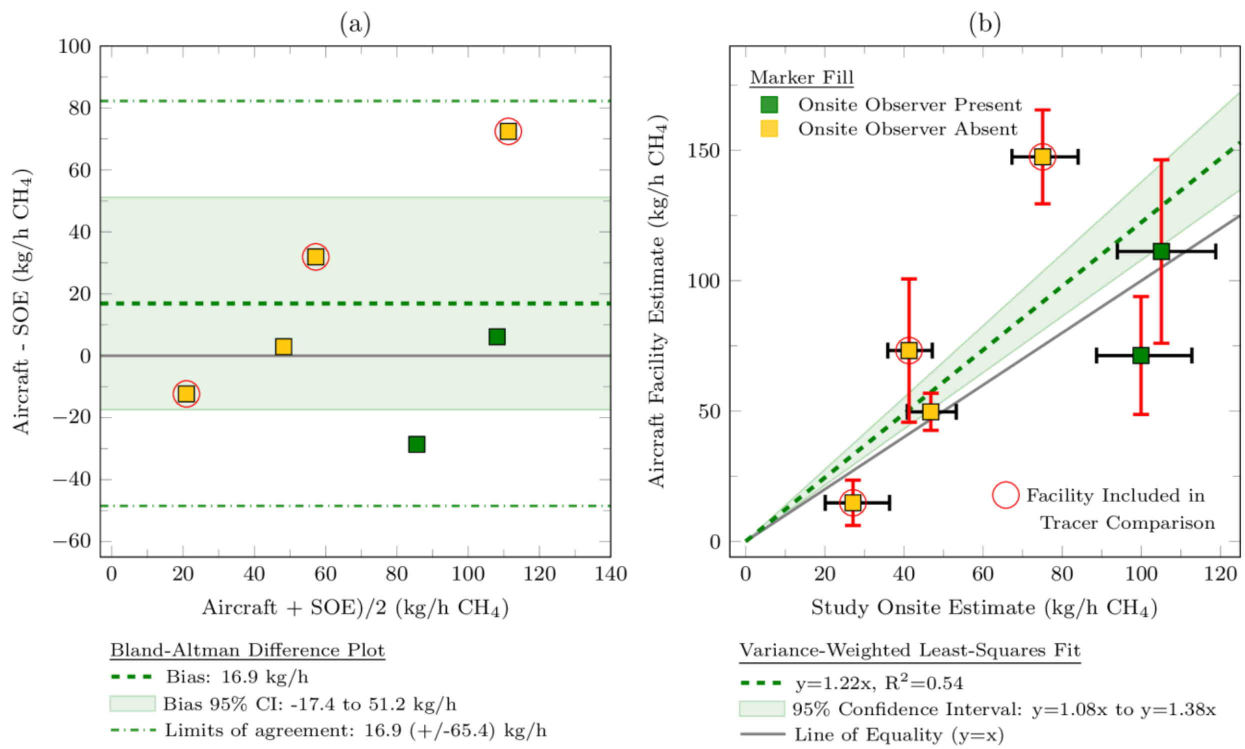

Figure S9: (a) Aircraft predicts higher facility-level CH_4 emission rates than SOE, but this result is not significant at the 95% confidence level. (b) Variance-weighted least-squares regression shows that aircraft predict higher facility-level CH_4 emission rates than study on-site estimates at the 95% confidence level.

In Figure S9(b) a VWLS regression (dashed line) is performed on aircraft and SOE. The slope of the regression (aircraft = 1.22·SOE, $R^2 = 0.54$) is greater than unity, indicating that aircraft predicts higher FLER than SOE. The 95% confidence interval (shaded region) on the regression slope (aircraft = 1.08·SOE to aircraft = 1.38·SOE) does not include the line of equality ($y = x$), indicating that aircraft predicts higher FLER than SOE at the 95% confidence level.

S7 Variance-weighted least-squares regression

The variance-weighted least-squares (VWLS) regression used in method comparisons employs the method described in Neri et al. (1989), and summarized here for convenience. Briefly, the sum of the squared orthogonal distances between each data point $P(x_i, y_i)$ and the line of best fit $y = ax + b$ (i.e. the VWLS fit) is minimized, accounting for the uncertainty δ (standard deviation) in both x and y data, $(\delta x_i, \delta y_i)$, by weighting each data point $P(x_i, y_i)$ by W_i . W_i is defined as the squared inverse of the orthogonal distance between the line of best fit and the data point, d_i:

$$W_i = \frac{1}{(\delta d_i)^2} \tag{1}$$

Where d_i is given by:

$$d_i = \frac{a x_i - y_i + b}{\sqrt{a^2 + 1}} \tag{2}$$

As illustrated in Figure S10.

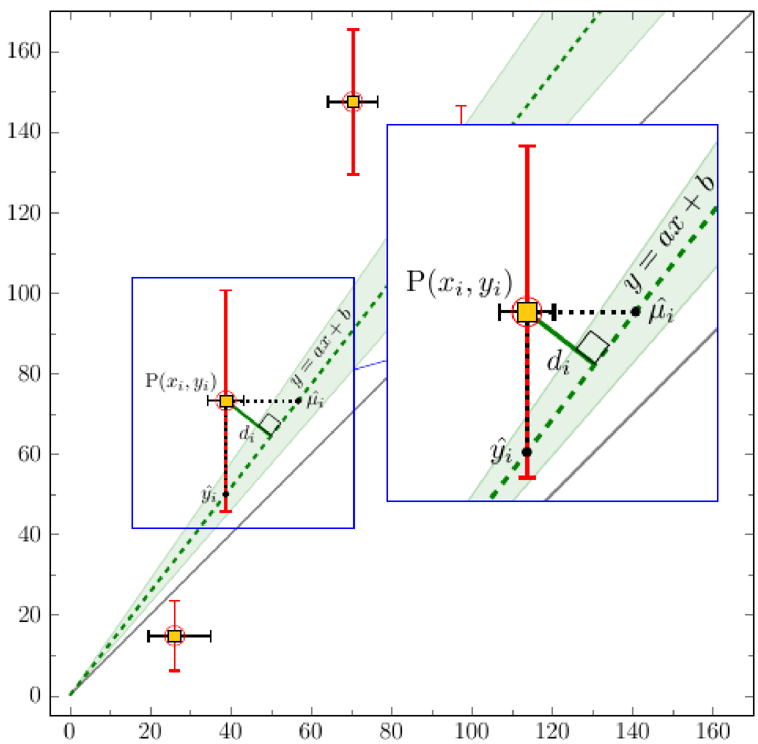

Figure S10: Example data point to illustrates variance-weighted least-squares technique.

By applying the propagation of error law to d_i:

$$\delta d_i = \frac{\partial d_i}{\partial x_i}\delta x_i + \frac{\partial d_i}{\partial y_i}\delta y_i = \frac{a}{\sqrt{a^2+1}}\delta x_i + \frac{1}{\sqrt{a^2+1}}\delta y_i \tag{3}$$

and assuming independent and random error; the error terms are added in quadrature to avoid an overestimate of the overall uncertainty:

$$(\delta d_i)^2 = \frac{a^2}{a^2+1}(\delta x_i)^2 + \frac{1}{a^2+1}(\delta y_i)^2 \tag{4}$$

The VWLS regression then becomes an exercise in minimizing F:

$$F = \sum_{i}^{N} \left(\frac{a x_i - y_i + b}{\sqrt{a^2 + 1}} \right)^2 \tag{5}$$

where each of the N experimental data points $P(x_i, y_i)$ are weighted by:

$$W_i = \frac{a^2 + 1}{a^2 (\delta x_i)^2 + (\delta y_i)^2} \tag{6}$$

The minimization is carried out using the bisection method outlined in Press et al. (1992) The minimization routine was implemented in C#, and was compared to the test case provided in Neri et al. (1989). The comparison indicated that the minimization routine was implemented successfully.

Table S5: VWLS regression minimization routine testing results, indicating successful test data reproduction.

Calculated value	Neri et al.	Present Paper	Exact Solution
a	-0.480 553 402 6	-0.480 533 407 446 273 49	-0.480 533 407
b	5.479 910 219 48	5.479 910 22 403 321 36	5.479 910 22

Additionally, we define a "total coefficient of determination" R^2 as:

$$R^2 = 1 - \frac{SSE}{SST} \tag{7}$$

Where SSE and SST include both x and y errors by defining:

$$SST = \sum (y_i - \bar{y})^2 + \sum (x_i - \bar{x})^2 \tag{8}$$

$$SSE = \sum (y_i - \hat{y}_i)^2 + \sum (x_i - \hat{\mu}_i)^2 \tag{9}$$

As illustrated in Figure S10.

S8 Comparison to GHGI

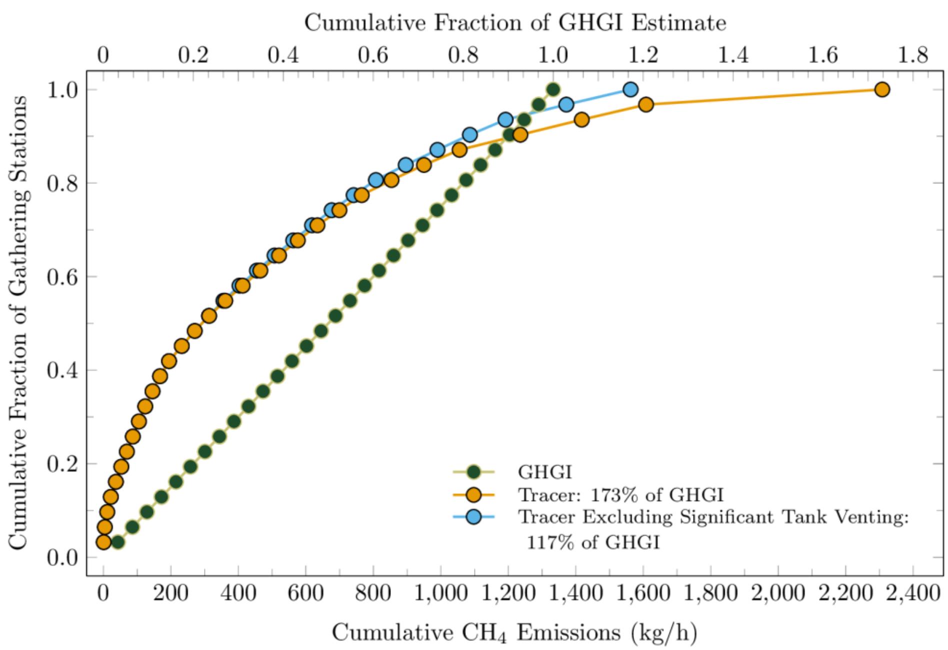

Figure S11: Cumulative fraction of tracer measurements compared to GHGI, both including and excluding tank venting emissions observed at two gathering stations.

Figure S11 compares the cumulative tracer measurements to the per-facility emission rate used for gathering stations in the EPA greenhouse gas inventory (GHGI) (53,066 scfd/day) (US EPA, 2016) or 43 kg/h. Significant tank venting was observed at gathering stations 33 and 121 (see S7). At station 121 tracer was able to quantify tank emissions, and at station 33 tank emissions were estimated by subtracting the SOE from the tracer measurement because the SOE captured all emissions except those emanating from the tank. The data series 'Tracer Excluding Significant Tank Venting' uses the SOE at these two facilities to account for emissions from those facilities other than tank venting. The data series 'Tracer' uses the tracer measurement from station 33, and adds the tank venting emission estimate made by tracer at station 121 to the SOE for station 121 to estimate a complete FLER. The average FLER for gathering stations measured by tracer in this study, *excluding* emissions from significant tank venting, is 50.4 kg/h, a 17% increase over the

GHGI per-facility estimate. The average FLER for gathering stations measured by tracer in this study, *including* emissions from significant tank venting, is 74.5 kg/h, a 73% increase over the GHGI per facility estimate.

S9 Simulated Direct Measurements (SDMs)

S9.1 Above Hi-Flow Range

In the event that an emission source was recorded at or above the measurable leak rate of the high-flow sampler, the measurement was removed from the ODM category, and was estimated by drawing a replacement emission rate from a right triangular distribution with maximum probability at the maximum measurable leak rate of the high-flow sampler (8 SCFM, 9.24kg/h) (Bacharach, Inc., 2015), tapering to a minimum probability at an emission rate of 16 SCFM (18.48 kg/h), and added to the SDM category. This upper limit was chosen on the assumption that on-site measurement personnel would not attempt to measure an emission source greater than twice the measurable leak rate, and conversely that any measurement attempt would capture at least half of the emission source. OGI camera observations reinforce that this is a reasonable assumption for the instances observed during this study. Figure S12 shows an image where qualitatively greater than half of the emission source was captured by the high-flow sampler.

Figure S12: Hi-Flow® over-range example still image taken from optical gas imaging (OGI) camera footage. In this case the emission rate exceeded the measurable leak rate, and was not capturing the entire emission plume.

S9.2 Below Hi-Flow Range

In the event that a measurement was observed with OGI, but registered below the measurable leak rate of the high-flow sampler (0.05 SCFM, 0.058 kg/h) (Bacharach, Inc., 2015), the measurement was removed from the ODM category, and was estimated by multiplying the measured reading by an uncertainty factor that increased from +/- 10% at the lower measurable leak rate to +/- 100% at recorded emission rate of 0 SCFM, and added to the SDM category.

S10 References

40 C.F.R. § 98.33. n.d. MANDATORY GREENHOUSE GAS REPORTING Subpart C—General Stationary Fuel Combustion Sources. Title 40: Protection of Environment PART 98 Electronic Code of Federal Regulations. Available at http://www.ecfr.gov/cgi-bin/text-idx?SID=e931cd0ca5c6798cca8f4da4c462dc52&mc=true&node=ap40.23.98_138.2&rgn=div9. Accessed 2017 Jan 22.

Bacharach, Inc. 2015. HI FLOW® Sampler For Natural Gas Leak Rate Measurement. Bacharach, Inc. Available at www.mybacharach.com/wp-content/uploads/2015/08/0055-9017-Rev-7.pdf. Accessed 2016 Jun 5.

Caterpillar. n.d. Caterpillar Application & Installation Guide Crankcase Ventilation Systems. Available at s7d2.scene7.com/is/content/Caterpillar/CM20160713-53120-62603. Accessed 2017 Mar 13.

Conley S, Faloona I, Mehrotra S, Suard M, Lenschow DH, Sweeney C, Herndon S, Schwietzke S, Pétron G, Pifer J, et al. 2017. (Under Review) Application of Gauss's Theorem to quantify localized surface emissions from airborne measurements of wind and trace gases. *Atmos Meas Tech Discuss* **2017**: 1–29. doi: 10.5194/amt-2017-55

GRI-GLYCalc Version 4.0. n.d. Available at http://sales.gastechnology.org/000102.html. Accessed 2017 Jan 21.

Johnson DR, Covington AN, Clark NN. 2015. Methane Emissions from Leak and Loss Audits of Natural Gas Compressor Stations and Storage Facilities. *Environ Sci Technol* **49**(13): 8132–8138. doi: 10.1021/es506163m

Myers D. 1996. Methane Emissions from the Natural Gas Industry, Volume 14: Glycol Dehydrators Final Report. Report No.: EPA 600/R-96-080n.

Neri F, Saitta G, Chiofalo S. 1989. An accurate and straightforward approach to line regression analysis of error-affected experimental data. *J Phys [E]* **22**(4): 215.

Press WH, editor. 1992. *Numerical Recipes in C: The Art of Scientific Computing*. 2nd ed. Cambridge ; New York: Cambridge University Press.

US EPA. 2016. Inventory of U.S. Greenhouse Gas Emissions and Sinks: 1990-2014, Annex 3. Washington, D.C. Report No.: EPA 430-R-16-002. Available at https://www3.epa.gov/climatechange/ghgemissions/usinventoryreport.html.

US EPA. n.d. Method 19 - Sulfur Dioxide Removal and Particulate, Sulfur Dioxide and Nitrogen Oxides from Electric Utility Steam Generators. Available at https://www.epa.gov/emc/method-19-sulfur-dioxide-removal-and-particulate-sulfur-dioxide-and-nitrogen-oxides-electric. Accessed 2017a Mar 10.

US EPA. n.d. Method 320 - Vapor Phase Organic and Inorganic Emissions by Extractive FTIR. Available at https://www.epa.gov/emc/method-320-vapor-phase-organic-and-inorganic-emissions-extractive-ftir. Accessed 2017b Jan 20.

US EPA. n.d. AP 42 Section 3.2 Natural Gas-fired Reciprocating Engines - Related Information|Technology Transfer Network | Emissions Factors and Policy Applications Center| US EPA. Available at http://www.epa.gov/ttn/chief/ap42/ch03/related/c03s02.html.

Yacovitch TI, Daube C, Vaughn TL, Bell CS, Roscioli JR, Knighton WB, Nelson DD, Zimmerle D, Pétron G, Herndon SC. 2017. (Submitted) Natural gas facility emission measurements by dual tracer flux in two US natural gas producing basins. *Elem Sci Anth*, in press.

Zavala-Araiza D, Alvarez RA, Lyon DR, Allen DT, Marchese AJ, Zimmerle DJ, Hamburg SP. 2017. Super-emitters in natural gas infrastructure are caused by abnormal process conditions. *Nat Commun* **8**: 14012. doi: 10.1038/ncomms14012